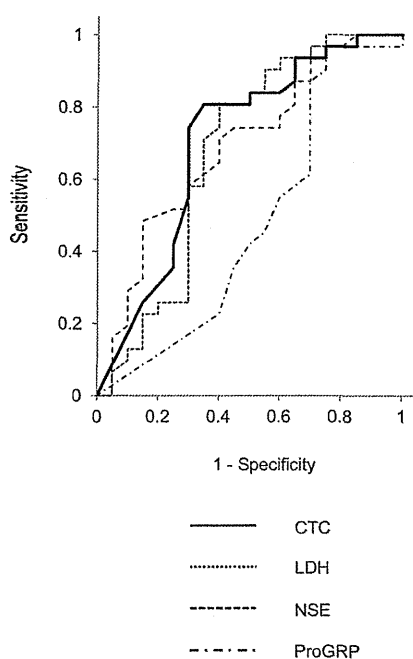


(0.29–0.64) for ProGRP. The differences in the AUROC among the parameters were not significant ( $p = 0.1044$ ).

### Radiologic Response and Changes in the CTC Levels

Assessment of the best radiologic response to the first-line treatment was performed using the RECIST criteria in 50 patients. One man died of interstitial lung disease before the follow-up imaging study. Figure 5 shows the baseline and posttreatment CTC levels in patients showing complete re-

sponse (CR,  $n = 6$ ), partial response (PR,  $n = 27$ ), stable disease (SD,  $n = 5$ ), and progressive disease (PD,  $n = 12$ ). There was no significant difference between the CR/PR subsets and SD/PD subsets in the baseline CTC (median, 4 [range, 0–1683] versus 4 [range, 0–5648];  $p = 0.7337$  by the Wilcoxon's test) or posttreatment CTC (0 [0–44] versus 0.5 [0–253];  $p = 0.3370$ ) level. The numbers of patients with undetectable posttreatment CTCs or patients with lower posttreatment CTC levels than the baseline CTC levels were 4 (66.7%) in the CR group, 24 (88.9%) in the PR group, 4 (80.0%) in the SD group, and 7 (58.3%) in the PD group, with no significant differences among the groups showing the various treatment responses ( $p = 0.2878$  by the  $\chi^2$  test).



**FIGURE 4.** Receiver operator characteristics curve analysis for predicting 1-year survivors. The area under the curve is 0.70 (95% confidence interval [CI], 0.52–0.83) for the circulating tumor cell (CTC) level at baseline, 0.67 (95% CI 0.49–0.82) for serum lactate dehydrogenase (LDH) at baseline, 0.68 (95% CI 0.52–0.82) for serum neuron-specific enolase (NSE) at baseline, and 0.46 (95% CI 0.29–0.64) for serum progastrin-releasing peptide (ProGRP) at baseline.

### DISCUSSION

This study is the first prospective evaluation of the optimal CTC cutoff to predict the OS in patients with chemotherapy-naïve SCLC. First, we showed that the CTC level was strongly predictive of the OS, especially in the ED subset. Then, an optimal cutoff level, CTC count of  $\geq 8$  cells per 7.5 ml of blood was identified by comparing the Cox proportional HRs of various CTC levels for the OS. This cutoff level was also found to be valid for predicting the posttreatment survival and postrelapse survival in the same cohort. We also showed that the baseline CTC level had a high discriminatory power, similar to the serum NSE and LDH.

Circulating SCLC cells have been reported to show high expression levels of EpCAM,<sup>19</sup> which has been used as a key marker to isolate CTCs using the CellSearch system. The appropriateness of using the CellSearch system for detecting circulating SCLC cells was previously assessed by Hou et al.<sup>16</sup> They showed that 15 CTC samples obtained from patients with SCLC by the CellSearch system were neuroendocrine in nature (CD56 positive) and confirmed their neoplastic origin by immunohistochemical comparison of these cells with the cells obtained from matched tumor biopsy specimens. The detection rate ( $\geq 2$  CTCs per 7.5 ml blood) of circulating SCLC cells by the CellSearch system in cases of SCLC is reportedly quite high, being 67 to 86%,<sup>8,16</sup> as compared with that in cases with other tumors with metasta-

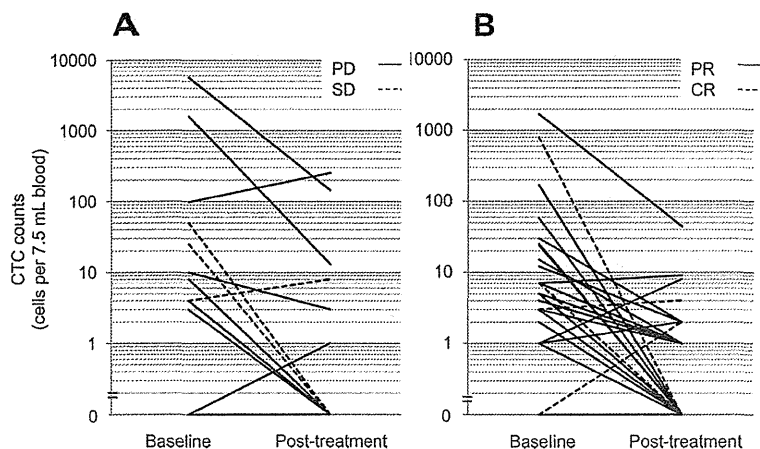


**FIGURE 5.** Relationship between radiologic response and the changes in the circulating tumor cell (CTC) level. A, Baseline and posttreatment CTC levels in patients showing PD (solid line) and SD (dotted line). B, Baseline and posttreatment CTC levels in patients showing PR (solid line) and CR (dotted line). PD, progressive disease; SD, stable disease; PR, partial response; CR, complete response.

ses.<sup>3,7,11,15</sup> Consistent with these reports, the detection rate in the SCLC patients in our study was 68.6%. Given that approximately half of our patients had nonmetastatic disease, we consider that CTCs are detected in a high percentage of cases of SCLC. Higher CTC counts have been reported as an indicator of the presence of distant metastases, such as bone metastasis in prostate cancer<sup>20</sup> and liver metastasis in colorectal cancer.<sup>11</sup> In patients with NSCLC, the CTC levels reportedly correlated with the number of organs showing metastatic involvement, and higher CTC levels are predictive of liver and bone metastasis.<sup>15</sup> Our results also showed an association between the CTC levels and the presence of metastasis, especially to the liver.

The CTC cutoff level (8 CTCs per 7.5 ml of blood) in our study to discriminate between groups with a favorable and unfavorable prognosis was higher than that reported for other tumors. In metastatic breast cancer, the cutoff level of 5 was chosen by comparing the median PFS and the Cox proportional HR for each threshold from 1 to 10,000 CTCs. The same cutoff was also shown to be correlated with the OS.<sup>7</sup> The cutoff of five cells was then applied to metastatic castration-resistant prostate cancer and was well validated to be predictive of the OS.<sup>14</sup> In metastatic colorectal cancer, the cutoff level of three cells was chosen by correlating the baseline CTC level with the response at the first follow-up imaging study. The cutoff level was well validated to be predictive of both the OS and PFS in a subsequent validation cohort.<sup>11</sup> Our cutoff level was based on a comparison of the Cox proportional HR for OS. The differences in the cutoff levels may be attributable to the statistical method used for choosing the optimal cutoff level or might reflect the highly metastatic potential of SCLC itself. In addition, we observed the prognostic significance of the baseline CTC only in the ED subset or patients treated by only chemotherapy in the subset analyses. As the previous studies in other malignancies have been conducted only in patients with metastatic disease, another study for ED-SCLC will be required to validate our results.

Conversion from an unfavorable baseline CTC level to a favorable follow-up CTC level reportedly has a strong impact on the survival. Patients with such conversion showed a favorable OS, statistically similar to that in patients with a persistent favorable CTC level in breast, prostate, and colorectal cancers.<sup>7,11,14</sup> In contrast, our study showed a relatively small impact of such conversion on the survival in SCLC patients. This difference might reflect the nature of SCLC itself, known to be aggressive and to rarely be in a dormant state.<sup>2,3</sup> A lower CTC level might be an appropriate treatment goal if minimal residual cancer cells after treatment had a larger impact on the survival in SCLC patients. Chemotherapeutic agents active against SCLC are as yet limited, and the classic platinum doublet with etoposide or irinotecan remains the standard first-line treatment regimen. Treatment options for relapsed SCLC are further limited to several cytotoxic agents,<sup>21,22</sup> and no molecular-targeted agents have yet been approved.<sup>23</sup> These limitations in treatment modalities might be related to the small impact of conversion after first-line treatment. NSE and ProGRP are commercially available

serum biomarkers and are used as markers for monitoring of SCLC patients. They have been reported to be highly sensitive and specific for the diagnosis of SCLC, and elevated levels of these markers at baseline have been shown to be associated with poor prognosis.<sup>24–26</sup> LDH has also been reported to have prognostic significance in patients of SCLC.<sup>27</sup> We showed that the baseline CTC level showed a good discriminatory power for predicting the prognosis in SCLC patients, similar to serum NSE and LDH, and furthermore, that the baseline CTC level was probably a better predictor of survival than the serum ProGRP, by receiver operator characteristics curve analysis.

The treatment response was reported to be associated with the CTC level at the time of imaging in breast cancer.<sup>28</sup> In colorectal cancer, the CTC level measured 3 to 5 weeks after the initiation of therapy had a relatively low sensitivity (27%) for predicting PD.<sup>11</sup> In our study, we found no correlation between the results of the response assessment using the RECIST criteria and the baseline CTC level, posttreatment CTC level, or change in the CTC level associated with treatment. The changes in the tumor size might not always be related to the changes in the outflow of tumor cells from the tumors.

The major limitation of this study was that the study population was small. The threshold value was derived from a cohort at a single institution and not validated in an independent validation cohort. In addition, our study included not only patients receiving chemotherapy alone but also patients treated by chemoradiotherapy. Because the treatment goals are different for chemotherapy and chemoradiotherapy, that is, palliation versus cure, separate derivation studies will be required to choose the optimal CTC cutoff level.

There has been an increasing interest in several aspects of CTCs. First, measurement of the CTC levels has been expected to guide decision making, such as determining the timing of changing, continuing, or discontinuing the current treatment, or identifying appropriate candidates for adjuvant chemotherapy.<sup>29–31</sup> Second, CTC analysis is anticipated to provide samples for biomarker analysis. Monitoring of human EGFR-related 2-positive CTCs in breast cancer patients during human EGFR-related 2-targeted therapy<sup>32–34</sup> and analysis of androgen receptor gene alterations in the CTCs of prostate cancer patients<sup>35,36</sup> have been reported. In addition, the newly developed CTC analyzer shows a high detection power for CTCs and was used for the analysis of *EGFR*-gene alterations in the CTCs from patients with NSCLC.<sup>37,38</sup> These studies have established a new role for CTC analysis as a noninvasive method of tumor profiling or target monitoring during treatment with molecular-targeted agents. Although few molecular-targeted agents currently available are active against SCLC, the high detection rate of CTCs in cases of SCLC might provide an opportunity for the screening of active drugs and accelerate the development of new therapeutic strategies.

In conclusion, this study showed that CTCs are readily detectable by the CellSearch system in patients with SCLC and that the CTC levels before and after treatment had strong

prognostic significance. A large prospective multiinstitutional validation study is required to confirm our results.

### ACKNOWLEDGMENTS

The authors thank Hiroaki Akamatsu, MD, Satoru Miura, MD, Madoka Kimura, MD, Rieko Kaira, MD, Sakae Morii, MD, Chikara Sakaguchi, MD, Hirofumi Eida, MD, Yoko Toda, MD, and Akihiro Tamiya, MD, for their constructive advice and provision of patients for this study.

### REFERENCES

- Jackman DM, Johnson BE. Small-cell lung cancer. *Lancet* 2005;366:1385–1396.
- Krug LM, Kris MG, Travis WD. Small cell and other neuroendocrine tumors of the lung. In DeVita VT, Lawrence TS, Rosenberg SA (Eds.). *CANCER Principles and Practice of Oncology*, 8th Ed. Philadelphia: Lipponcott Williams & Wilkins, 2008. Pp. 946–963.
- Allard WJ, Matera J, Miller MC, et al. Tumor cells circulate in the peripheral blood of all major carcinomas but not in healthy subjects or patients with nonmalignant diseases. *Clin Cancer Res* 2004;10:6897–6904.
- Fetsch PA, Cowan KH, Weng DE, et al. Detection of circulating tumor cells and micrometastases in stage II, III, and IV breast cancer patients utilizing cytology and immunocytochemistry. *Diagn Cytopathol* 2000;22:323–328.
- Loberg RD, Fridman Y, Pienta BA, et al. Detection and isolation of circulating tumor cells in urologic cancers: a review. *Neoplasia* 2004;6:302–309.
- Molnar B, Sipos F, Galamb O, et al. Molecular detection of circulating cancer cells. Role in diagnosis, prognosis and follow-up of colon cancer patients. *Dig Dis* 2003;21:320–325.
- Cristofanielli M, Budd GT, Ellis MJ, et al. Circulating tumor cells, disease progression, and survival in metastatic breast cancer. *N Engl J Med* 2004;351:781–791.
- Tanaka F, Yoneda K, Kondo N, et al. Circulating tumor cell as a diagnostic marker in primary lung cancer. *Clin Cancer Res* 2009;15:6980–6986.
- Kagan M, Howard D, Bendele T, et al. A sample preparation and analysis system for identification of circulating tumor cells. *J Clin Ligand Assay* 2002;25:104–110.
- Riethdorf S, Fritsche H, Muller V, et al. Detection of circulating tumor cells in peripheral blood of patients with metastatic breast cancer: a validation study of the CellSearch system. *Clin Cancer Res* 2007;13:920–928.
- Cohen SJ, Punt CJ, Iannotti N, et al. Relationship of circulating tumor cells to tumor response, progression-free survival, and overall survival in patients with metastatic colorectal cancer. *J Clin Oncol* 2008;26:3213–3221.
- Cohen SJ, Punt CJ, Iannotti N, et al. Prognostic significance of circulating tumor cells in patients with metastatic colorectal cancer. *Ann Oncol* 2009;20:1223–1229.
- Cristofanielli M, Hayes DF, Budd GT, et al. Circulating tumor cells: a novel prognostic factor for newly diagnosed metastatic breast cancer. *J Clin Oncol* 2005;23:1420–1430.
- de Bono JS, Scher HI, Montgomery RB, et al. Circulating tumor cells predict survival benefit from treatment in metastatic castration-resistant prostate cancer. *Clin Cancer Res* 2008;14:6302–6309.
- Krebs MG, Sloane R, Priest L, et al. Evaluation and prognostic significance of circulating tumor cells in patients with non-small-cell lung cancer. *J Clin Oncol* 2011;29:1556–1563.
- Hou JM, Greystoke A, Lancashire L, et al. Evaluation of circulating tumor cells and serological cell death biomarkers in small cell lung cancer patients undergoing chemotherapy. *Am J Pathol* 2009;175:808–816.
- Wu C, Hao H, Li L, et al. Preliminary investigation of the clinical significance of detecting circulating tumor cells enriched from lung cancer patients. *J Thorac Oncol* 2009;4:30–36.
- Eisenhauer EA, Therasse P, Bogaerts J, et al. New response evaluation criteria in solid tumours: revised RECIST guideline (version 1.1). *Eur J Cancer* 2009;45:228–247.
- Kularatne BY, Lorigan P, Browne S, et al. Monitoring tumour cells in the peripheral blood of small cell lung cancer patients. *Cytometry* 2002;50:160–167.
- Scher HI, Jia X, de Bono JS, et al. Circulating tumour cells as prognostic markers in progressive, castration-resistant prostate cancer: a reanalysis of IMMC38 trial data. *Lancet Oncol* 2009;10:233–239.
- Inoue A, Sugawara S, Yamazaki K, et al. Randomized phase II trial comparing arubicin with topotecan in patients with previously treated small-cell lung cancer: North Japan Lung Cancer Study Group Trial 0402. *J Clin Oncol* 2008;26:5401–5406.
- von Pawel J, Schiller JH, Shepherd FA, et al. Topotecan versus cyclophosphamide, doxorubicin, and vincristine for the treatment of recurrent small-cell lung cancer. *J Clin Oncol* 1999;17:658–667.
- Puglisi M, Dolly S, Faria A, et al. Treatment options for small cell lung cancer - do we have more choice? *Br J Cancer* 2010;102:629–638.
- Nisman B, Biran H, Ramu N, et al. The diagnostic and prognostic value of ProGRP in lung cancer. *Anticancer Res* 2009;29:4827–4832.
- Wójcik E, Kulpa JK, Sas-Korczyńska B, et al. ProGRP and NSE in therapy monitoring in patients with small cell lung cancer. *Anticancer Res* 2008;28:3027–3033.
- Shibayama T, Ueoka H, Nishii K, et al. Complementary roles of pro-gastrin-releasing peptide (ProGRP) and neuron specific enolase (NSE) in diagnosis and prognosis of small-cell lung cancer (SCLC). *Lung Cancer* 2001;32:61–69.
- Albain KS, Crowley JJ, LeBlanc M, et al. Survival determinants in extensive-stage non-small-cell lung cancer: the Southwest Oncology Group experience. *J Clin Oncol* 1991;9:1618–1626.
- Liu MC, Shields PG, Warren RD, et al. Circulating tumor cells: a useful predictor of treatment efficacy in metastatic breast cancer. *J Clin Oncol* 2009;27:5153–5159.
- Lin H, Balic M, Zheng S, et al. Disseminated and circulating tumor cells: role in effective cancer management. *Crit Rev Oncol Hematol* 2011;77:1–11.
- Roukos DH, Murray S, Briassoulis E. Molecular genetic tools shape a roadmap towards a more accurate prognostic prediction and personalized management of cancer. *Cancer Biol Ther* 2007;6:308–312.
- Wicha MS, Hayes DF. Circulating tumor cells: not all detected cells are bad and not all bad cells are detected. *J Clin Oncol* 2011;29:1508–1511.
- Fehm T, Muller V, Aktas B, et al. HER2 status of circulating tumor cells in patients with metastatic breast cancer: a prospective, multicenter trial. *Breast Cancer Res Treat* 2010;124:403–412.
- Ignatiadis M, Rothe F, Chaboteaux C, et al. HER2-positive circulating tumor cells in breast cancer. *PLoS One* 2011;6: e15624.
- Riethdorf S, Muller V, Zhang L, et al. Detection and HER2 expression of circulating tumor cells: prospective monitoring in breast cancer patients treated in the neoadjuvant GeparQuattro trial. *Clin Cancer Res* 2010;16:2634–2645.
- Jiang Y, Palma JF, Agus DB, et al. Detection of androgen receptor mutations in circulating tumor cells in castration-resistant prostate cancer. *Clin Chem* 2010;56:1492–1495.
- Leversha MA, Han J, Asgari Z, et al. Fluorescence in situ hybridization analysis of circulating tumor cells in metastatic prostate cancer. *Clin Cancer Res* 2009;15:2091–2097.
- Maheswaran S, Sequist LV, Nagrath S, et al. Detection of mutations in EGFR in circulating lung-cancer cells. *N Engl J Med* 2008;359:366–377.
- Nagrath S, Sequist LV, Maheswaran S, et al. Isolation of rare circulating tumour cells in cancer patients by microchip technology. *Nature* 2007;450:1235–1239.



Published in final edited form as:

Ann Surg Oncol. 2012 July ; 19(Suppl 3): 634–645. doi:10.1245/s10434-011-2142-0.

## Transient but Not Stable *ZEB1* Knockdown Dramatically Inhibits Growth of Malignant Pleural Mesothelioma Cells

Mihoko Horio, MD<sup>1</sup>, Mitsuo Sato, MD, PhD<sup>1</sup>, Yoshihiro Takeyama, MD, PhD<sup>1</sup>, Momen Elshazley, MD, MSc<sup>1</sup>, Ryo Yamashita, MD<sup>1</sup>, Tetsunari Hase, MD<sup>1</sup>, Kenya Yoshida, MD<sup>1</sup>, Noriyasu Usami, MD, PhD<sup>2</sup>, Kohei Yokoi, MD, PhD<sup>2</sup>, Yoshitaka Sekido, MD, PhD<sup>3,5</sup>, Masashi Kondo, MD, PhD<sup>1</sup>, Shinya Toyokuni, MD, PhD<sup>4</sup>, Adi F. Gazdar, MD<sup>6</sup>, John D. Minna, MD<sup>6</sup>, and Yoshinori Hasegawa, MD, PhD<sup>1</sup>

<sup>1</sup>Department of Respiratory Medicine, Nagoya University Graduate School of Medicine, Nagoya, Japan

<sup>2</sup>Division of Thoracic Surgery, Nagoya University Graduate School of Medicine, Nagoya, Japan

<sup>3</sup>Department of Cancer Genetics, Nagoya University Graduate School of Medicine, Nagoya, Japan

<sup>4</sup>Department of Pathology and Biological Responses, Nagoya University Graduate School of Medicine, Nagoya, Japan

<sup>5</sup>Division of Molecular Oncology, Aichi Cancer Center Research Institute, Nagoya, Japan

<sup>6</sup>Hamon Center for Therapeutic Oncology Research and the Simmons Comprehensive Cancer Center, University of Texas Southwestern Medical Center at Dallas, Dallas, TX

### Abstract

**Background**—The role of *ZEB1*, a master epithelial-to-mesenchymal transition gene, in malignant pleural mesothelioma (MPM) is unclear.

**Methods**—The expression of *ZEB1*, E-cadherin, vimentin, and epithelial cell adhesion molecule (*EpCAM*) in 18 MPM cell lines and a normal pleural mesothelial cell line MeT-5A was determined by quantitative real-time polymerase chain reaction and Western blot testing. RNA interference-mediated transient and/or stable knockdown of *ZEB1* and *EpCAM* was performed. Microarray expression analysis was performed with a TORAY-3D gene chip. Growth was evaluated by colorimetric proliferation and colony formation assays. Luciferase reporter assay was performed to access the effects of *ZEB1* knockdown on *EpCAM* promoter activity.

**Results**—Most MPM cell lines exhibited mesenchymal phenotype and expressed *ZEB1*. Transient *ZEB1* knockdown suppressed growth in all four cell lines studied (ACC-MESO-1, H2052, Y-MESO-8A, Y-MESO-29) while stable *ZEB1* knockdown suppressed growth only in Y-MESO-29. Genome-wide gene expression analysis revealed that *EpCAM* was the most prominently up-regulated gene by both transient and stable *ZEB1* knockdown in ACC-MESO-1, with more marked up-regulation in stable knockdown. We hypothesized that *EpCAM* up-regulation counteracts the stable *ZEB1* knockdown-induced growth inhibition in ACC-MESO-1. Transient *EpCAM* knockdown suppressed growth dramatically in ACC-MESO-1 cells expressing sh*ZEB1* but only modestly in those expressing sh*GFP*, supporting our hypothesis. Luciferase

© Society of Surgical Oncology 2011

M. Sato, MD, PhD, msato@med.nagoya-u.ac.jp.

**Electronic supplementary material** The online version of this article (doi:10.1245/s10434-011-2142-0) contains supplementary material, which is available to authorized users.

reporter assay showed that *ZEB1* knockdown resulted in increased *EpCAM* promoter activity. *EpCAM* was also up-regulated in Y-MESO-29 expressing sh*ZEB1*, but this *EpCAM* up-regulation did not counteract *ZEB1* knockdown-induced growth suppression, suggesting that the counteracting effects of *EpCAM* may be cellular context dependent.

**Conclusions**—RNA interference-mediated *ZEB1* knockdown may be a promising therapeutic strategy for MPM, but one has to consider the possibility of diminished growth inhibitory effects of long-term *ZEB1* knockdown, possibly as a result of *EpCAM* up-regulation and/or other gene expression changes resulting from *ZEB1* knockdown.

Malignant pleural mesothelioma (MPM) is a highly aggressive tumor arising from the mesothelium lining the pleural surface, mostly resulting from occupational exposure to asbestos fibers.<sup>1,2</sup> The disease progresses rapidly and is highly resistant to current therapeutic modalities comprising chemotherapy, radiotherapy, and surgery, and therefore the overall survival is extremely poor, with the median survival being 9 to 17 months.<sup>2</sup> Two thousand to 3000 new MPM cases occur yearly in the United States, and the incidence of this disease is predicted to continue rising for the next two decades. Thus, it is imperative to develop novel therapeutics for MPM that target the molecules commonly altered in MPM.

Malignant cells of epithelial origin often lose their epithelial phenotype and acquire fibroblastic characteristics during disease progression.<sup>3</sup> This process is referred to as the epithelial-to-mesenchymal transition (EMT). EMT was originally discovered as an embryonic developmental program involving drastic changes in cell morphology as well as expression of EMT-associated genes. EMT occurs during the progression of several types of human epithelial cancers and confers motility and invasiveness on the cells, leading them to acquire the ability to metastasize to distant sites. MPM originates in normal pleural mesothelial cells, which derive from mesodermal (mesenchymal) cells, and one could hypothesize that the mesodermal origin of MPM contributes to its aggressive behavior.<sup>4</sup> In support of this hypothesis, MPM tumors often show epithelial histological features, which correlates with a favorable patient prognosis.<sup>1</sup>

Several master EMT regulator genes encoding transcription factors, including *Twist*, *Snail*, *Slug*, *ZEB1*, *SIP*, and *Gooseoid*, have been identified, and their roles in epithelial cancers have been demonstrated.<sup>5</sup> Among them, *ZEB1* is increasingly considered to be a key player in the progression of epithelial cancers. *ZEB1* promotes tumor metastasis in colon and breast cancer and enhances transendothelial migration in prostate cancer cells.<sup>6</sup> In addition, we recently showed that transient knockdown of *ZEB1* in lung cancer greatly suppresses anchorage-independent growth of lung cancer cells.<sup>7</sup>

With this background, we aimed to study the role of *ZEB1* in the pathogenesis of MPM. To this end, we performed transient and stable knockdown of *ZEB1* and evaluated its effects on the growth of MPM.

## MATERIALS AND METHODS

### Cell Lines and Tissue Culture

Eighteen MPM cell lines (H28, H290, H2052, H2373, H2452, Y-MESO-8A, Y-MESO-8D, Y-MESO-9, Y-MESO-12, Y-MESO-14, Y-MESO-21, Y-MESO-22, Y-MESO-25, Y-MESO-26B, Y-MESO-29, MASTO-211H, ACC-MESO-1, ACC-MESO-4) and one lung cancer cell line (HI299) used in this study were purchased from American Type Culture Collection (ATCC, Manassas, VA) or obtained from the Aichi Cancer Center or University of Texas Southwestern Medical Center collections.<sup>8</sup> These cells were cultured with RPMI 1640 (Sigma-Aldrich, St. Louis, MO) supplemented with 10% fetal bovine serum. The nontumorigenic mesothelial cell line MeT-5A, which was established by introduction of

SV40 large T antigen into normal epithelial cells, was purchased from ATCC and used as a normal control line.<sup>9</sup> MeT-5A cells were cultured in Medium 199 with Earle's BSS, 0.75 mM L-glutamine, and 1.25 g/L sodium bicarbonate supplemented with 3.3 nM epidermal growth factor, 400 nM hydrocortisone, 870 nM insulin 20 mM HEPES, and 10% fetal bovine serum.

### RNA Isolation and Quantitative Real-Time Polymerase Chain Reaction Analysis

Five micrograms of total RNA isolated with Trizol (Invitrogen, Carlsbad, CA) were reverse transcribed with a Superscript III First-Strand Synthesis System with a Random primer system (Invitrogen). Quantitative real-time polymerase chain reaction (qRT-PCR) of *E-cadherin*, *vimentin*, *ZEB1*, and *EpCAM* was performed as described previously with the standard TaqMan assay-on-demand PCR protocol in a reaction volume of 20  $\mu$ L, including 1  $\mu$ L cDNA (10). We used the comparative  $C_t$  method to compute relative expression values. We used *GAPDH* (Applied Biosystems assay-on-demand) as an internal control.

### Western Blot Analysis

Western blot analysis was performed as described previously with whole cell lysates.<sup>10</sup> Primary antibodies used were mouse monoclonal anti-E-cadherin, anti-vimentin (BD Bioscience, Franklin Lakes, NJ), goat polyclonal anti-ZEB1 (Santa Cruz Biotechnology, Santa Cruz, CA), rabbit polyclonal anti-cleaved caspase 3 (Cell Signaling Technology, Danvers, MA), mouse monoclonal anti-EpCAM (Thermo Fisher Scientific, Waltham, MA) and mouse monoclonal anti-actin (Sigma) antibodies. Actin protein was used as a control for adequacy of equal protein loading. Anti-rabbit, anti-mouse (GE Healthcare, Buckinghamshire, England), or anti-goat antibody (R&D Systems, Minneapolis, MN) was used at a 1:2000 dilution as a secondary antibody.

### Transfection of Short Interfering RNA

Cells ( $4.5 \times 10^5$ ) were plated in six-well plates. The next day, the cells were transiently transfected with either 10 nM predesigned short interfering RNA (siRNA) (Stealth Select RNAi) targeting *ZEB1*, *EpCAM*, or a control siRNA purchased from Invitrogen with Lipofectamine RNAiMAX (Invitrogen) according to the manufacturer's protocol. After 48 h, the transfected cells were collected for further analyses or plated for cell growth assays.

### Transfection of shRNA Expressing Retroviral Vectors

pSUPER.retro.ZEB1 and pSUPER.retro.GFP control vectors were kindly provided by Dr. Thomas Brabletz.<sup>11</sup> Virus-containing medium was produced as described previously.<sup>10</sup> Target cells were transduced by retrovirus-containing medium and then underwent drug selection with puromycin for 3 to 5 days.

### Cell Growth Assay

A colorimetric proliferation assay was performed with a WST-1 assay kit (Roche, Basel, Switzerland) according to the manufacturer's instructions. Liquid and soft agar colony formation assays were done as described previously.<sup>10</sup>

### Cell Cycle Analysis

Cells were collected 48 h after the transfection of siRNA oligos. Cells were fixed in 70% ethanol, treated with RNase A, stained with propidium iodide with a BD Cycletest Plus Reagent Kit (BD Bioscience) according to the instructions of the manufacturer, and analyzed by flow cytometry for DNA synthesis and cell cycle status (FACSCalibur cell sorter, Becton Dickinson) with BD Cell Quest Pro version 5.2.1 (BD Bioscience).

### Microarray Expression Analysis

For DNA microarray analysis, a 3D-Gene Human Oligo chip 25 k (Toray Industries, Tokyo, Japan) was used (25,370 distinct genes). Additional details of microarray analysis are described in the Supplemental Information.

### Senescence-Associated $\beta$ -Galactosidase Staining

Cells were stained with  $\beta$ -galactosidase with a Senescence  $\beta$ -Galactosidase Staining Kit (Cell Signaling Technology), and cells stained blue were counted under a microscope ( $\times 200$  total magnification).

### Immunohistochemistry

Surgically resected 15 primary MPM tumor and four normal parietal pleura samples were obtained from patients at Nagoya University Hospital. Before tissue samples were collected ethical approval and fully informed written consent from all patients were obtained. Immunohistochemistry of ZEB1 was performed using standard techniques with some modifications. Additional details of immunohistochemistry analysis are described in Supporting Information.

### Luciferase Reporter Assay

Cells were transfected with ZEB1 or control siRNA oligos. Next day, the transfected cells were replated in 96-well plates and then transfected with TACSTD1 (EpCAM)-PROM firefly luciferase vector (Switchgear) containing entire promoter region of EpCAM or pGL4.11 control vector (Promega) and phRL-TK renilla luciferase vector. Forty-eight hours after transfection, reporter gene activities were determined by a luminometer with Dual-Luciferase reporter assay system (Promega). Reporter activity was normalized by calculating the ratio of firefly/renilla values.

### Statistical Analysis

SPSS version 18 software (SPSS, Chicago, IL) was used for all statistical analyses in this study. The Mann-Whitney *U*-test was used for analyzing differences between two groups.

## RESULTS

### The majority of MPM cell lines exhibit mesenchymal phenotype (low E-cadherin/high vimentin) and express ZEB1

We performed qRT-PCR and Western blot testing of ZEB1, vimentin (a mesenchymal marker), E-cadherin (an epithelial marker), and epithelial cell adhesion molecule (EpCAM) for 18 MPM cell lines and MeT-5A, a nontumorigenic mesothelial cell line, used as a normal control. The majority of MPM lines expressed undetectable to very low levels of E-cadherin and high levels of vimentin, which probably reflects the mesodermal origin of MPM (Fig. 1a). ZEB1 directly inhibits E-cadherin expression, and an inverse correlation between their expressions has been shown in several different types of human cancers.<sup>7,12</sup> However, we did not see a correlation between E-cadherin and ZEB1 expression (Fig. 1a, b). Only two cell lines (Y-MESO-12, Y-MESO-29) expressed detectable levels of EpCAM protein (Fig. 1c).

### Transient ZEB1 Knockdown Induces Re-expression of E-cadherin in ACC-MESO-1 but Not in H2052

To see whether ZEB1 expression plays a role in inhibiting E-cadherin expression in MPM cells, we performed transient knockdown of ZEB1 using prevalidated synthesized siRNA

oligos (Invitrogen) in two mesothelioma lines, ACC-MESO-1 and H2052, which express high and moderate levels of *ZEB1* mRNA, respectively (Fig. 1b). The two cell lines were transiently transfected with each of the three *ZEB1* siRNA or control oligos and collected 48 h after transfection for protein expression analyses. Western blot testing of *ZEB1* showed that clear suppression of *ZEB1* protein by all three siRNA oligos was obtained in the two lines (Fig. 2a). After the *ZEB1* knockdown, E-cadherin protein was re-expressed in ACC-MESO-1 but not in H2052. A previous study reported that the promoter region of *E-cadherin* is heavily methylated in H2052 cells, which results in silenced *E-cadherin* expression in the cells.<sup>13</sup> Thus, it is likely that the loss of *ZEB1* expression was unable to overcome this methylation-mediated gene silencing in H2052 cells. *Vimentin* expression did not change in either of the lines (Fig. 2a). We did not observe marked morphological changes in either of the cell lines after the transient *ZEB1* knockdown.

### Transient ZEB1 Knockdown Induces Suppression of Proliferation, Anchorage-Dependent, and Anchorage-Independent Clonal Growth in MPM Cells

To test the effects of *ZEB1* knockdown on cell proliferation in mass culture, we did colorimetric growth assays. Two days after the transfection of *ZEB1* siRNA oligos, ACC-MESO-1 and H2052 cells were plated for growth assays. *ZEB1* knockdown suppressed proliferation in the two cell lines compared to control cells (Fig. 2b). To examine the effect of *ZEB1* knockdown on the clonogenic growth of MPM cells in anchorage-dependent and -independent conditions, we performed liquid and soft agar colony formation assays, respectively. In both assays, *ZEB1* knockdown dramatically suppressed colony formation in the two cell lines (Fig. 2c, d). To evaluate cell death rate due to “off-target” effects in cells transfected with control siRNA, we included cells transfected with transfection reagent only in the proliferation and liquid colony formation experiments and we did not see statistically significant differences in cell death rates between these two treatment groups (data not shown), indicating that cell death rates due to “off-target” effects in the controls were very low. To see whether such dramatic growth inhibitory effects of transient *ZEB1* knockdown are also seen in MPM cell lines that express *ZEB1* at low levels, we did transient *ZEB1* knockdown for Y-MESO-8A and Y-MESO-29, which express *ZEB1* mRNA at very low levels (*ZEB1* protein was not detectable) (Fig. 1b). Efficient *ZEB1* knockdown in these cell lines was confirmed by qRT-PCR (Fig. 2e). The knockdown dramatically suppressed their liquid colony formation (Fig. 2f), suggesting that low levels of *ZEB1* expression also have roles in the growth of MPM cells. In addition, we performed *ZEB1* knockdown in MeT-5A cells. *ZEB1* knockdown suppressed proliferation of MeT-5A to ~50% while the knockdown only marginally suppressed its liquid colony formation (Fig. 2g), suggesting that MPM cell lines are more dependent on their growth for *ZEB1* expression than their normal counterpart cell line. To explore the mechanism underlying the growth inhibition by *ZEB1* knockdown in the MPM cell lines we performed apoptosis, cell cycle, and senescence analyses in ACC-MESO-1 and H2052. However, we did not see any differences between *ZEB1* knockdown and control cells in any of the assays (data not shown). To gain insights into underlying mechanisms of growth inhibition by transient *ZEB1* knockdown we performed genome-wide gene expression analysis for ACC-MESO-1 cells transfected with *ZEB1* or control siRNA oligos. Genes more than 4-fold up- and down-regulated are shown in Tables 1 and 2, respectively. Several genes known to have oncogenic roles were down-regulated by more than 2-fold in *ZEB1* knockdown cells compared to control, including *KRAS*, *Interleukin 6*,  $\beta$ -*catenin*, *cyclin E*, and *caveolin 1*.<sup>14,15</sup> Conversely, *PTEN*, a well-known tumor suppressor gene was up-regulated by more than 2-fold in *ZEB1* knockdown cells.<sup>6</sup> These expression changes may contribute to growth inhibitory effects of *ZEB1* knockdown.



### Stable Knockdown of ZEB1 Induces Morphological Changes Suggestive of Mesenchymal-to-Epithelial Transition (MET) in ACC-MESO-1 Cells

To evaluate the long-term effects of *ZEB1* knockdown on growth as well as cellular morphology in MPM cells, we performed stable *ZEB1* knockdown with a retroviral short hairpin RNA (shRNA)-expressing vector. ACC-MESO-1, H2052, Y-MESO-8A, and Y-MESO-29 cells were transfected with a sh*ZEB1*- or sh*GFP*-expressing vector and underwent drug selection. Stable *ZEB1* knockdown resulted in *E-cadherin* re-expression in ACC-MESO-1, Y-MESO-8A, and Y-MESO-29 but not in H2052 while *vimentin* expression remained unchanged in all the cell lines (Fig. 3a). Stable *ZEB1* knockdown caused ACC-MESO-1 to undergo morphological changes suggestive of a mesenchymal-to-epithelial (MET) transition; ACC-MESO-1 cells changed their morphology from an elongated spindle-like (fibroblastic) shape with a scattered growth pattern to a rounded epithelial-like shape with a cobblestone-like growth pattern (Fig. 3b). These morphological changes together with the *E-cadherin* re-expression after *ZEB1* knockdown suggest that *ZEB1* expression contributes to maintaining the mesenchymal phenotype in ACC-MESO-1. MET-like morphological changes were not seen in other cell lines after stable *ZEB1* knockdown.

### Stable ZEB1 Knockdown Shows Only Modest Growth Suppression in MPM Cells

To evaluate the effects of stable *ZEB1* knockdown on the growth of MPM cells, we performed WST-1 proliferation and liquid and soft agar colony formation assays on ACC-MESO-1 and H2052 cells expressing sh*ZEB1* or sh*GFP*. WST-1 and liquid colony formation assays showed no or only a slight difference between sh*ZEB1* and sh*GFP*-expressing cells in the cell lines (Fig. 3c, d). Soft agar colony formation assays showed that the stable *ZEB1* knockdown suppressed colony formation in ACC-MESO-1 but not in H2052 cells (Fig. 3e). We also performed liquid colony formation assay for *ZEB1* low-expressing cells (ACC-MESO-8A, ACC-MESO-29). Stable *ZEB1* knockdown suppressed liquid colony formation to ~80% in ACC-MESO-8A and to ~30% in ACC-MESO-29 compared to controls (Fig. 3f). These results indicate that stable *ZEB1* knockdown suppressed growth of MPM cells to a lesser extent compared to transient *ZEB1* knockdown, suggesting that other factors may diminish growth inhibitory effects of *ZEB1* knockdown in these cells.

### Diminished growth inhibition of stable ZEB1 knockdown in ACC-MESO-1 cells is in part attributed to up-regulation of EpCAM resulting from ZEB1 knockdown

To explore genes that may contribute to diminished growth inhibitory effects of stable *ZEB1* knockdown we performed genome-wide gene expression analysis of stable *ZEB1* knockdown ACC-MESO-1 cells and compared its results with those of transient *ZEB1* knockdown cells (Tables 1 and 2). Of note, *EpCAM* was the most prominently up-regulated genes in both transient and stable *ZEB1* knockdown experiments, with more marked up-regulation in stable knockdown (6.6 times more up-regulated in stable knockdown than in transient knockdown). Oncogenic roles of *EpCAM* are well-demonstrated by several groups including us.<sup>17-19</sup> Thus, we hypothesized that this marked *EpCAM* up-regulation by stable *ZEB1* knockdown may in part contribute to the diminished growth inhibition by stable *ZEB1* knockdown in ACC-MESO-1 cells. To test this hypothesis, we examined whether *EpCAM* knockdown inhibits growth of sh*ZEB1*-expressing ACC-MESO-1. *EpCAM* knockdown dramatically suppressed liquid colony formation in sh*ZEB1*-expressing ACC-MESO-1 cells but only modestly suppressed in those expressing sh*GFP* (Fig. 4). These results suggest that *EpCAM* up-regulation induced by stable *ZEB1* knockdown may in part account for the diminished growth inhibitory effects of stable *ZEB1* knockdown in ACC-MESO-1 cells. Nevertheless, this finding was not generalized to other cell lines. Y-MESO-8A, which also showed no growth suppression by stable *ZEB1* knockdown (Fig. 3f), did not up-regulate *EpCAM* expression after stable *ZEB1* knockdown (Fig. 3a). In addition,

Y-MESO-29 showed growth suppression by stable *ZEB1* knockdown (Fig. 3f) although it showed *EpCAM* up-regulation by stable *ZEB1* knockdown (Fig. 3a). These suggest that the counteracting effects of *EpCAM* may be cellular context-dependent and that other gene expression changes resulting from *ZEB1* knockdown may also contribute to the diminished growth inhibition.

### ZEB1 Suppresses *EpCAM* Expression through Repressing *EpCAM* Promoter Activity

To see whether *ZEB1* knockdown-induced *EpCAM* up-regulation results from induction of promoter activity, we performed luciferase reporter assay. We used H1299 lung cancer cell line because it can be easily transfected with plasmid DNA. H1299 cells were transfected with *ZEB1* or control siRNA oligos, and then transfected with *EpCAM* promoter containing luciferase vector or promoterless control vector (pGL4.11) and phRL-TK vector. *EpCAM* transcription activity was higher in H1299 cells transfected with *ZEB1* siRNA oligos than in those transfected with control siRNA oligos, demonstrating that *ZEB1* knockdown-induced *EpCAM* up-regulation results from induction of promoter activity (Fig. 5).

### ZEB1 Protein Is Expressed in a Substantial Fraction of Human MPM Tissue Sections

We analyzed *ZEB1* protein expression in 15 clinical MPM samples as well as four normal parietal pleural samples by immunohistochemistry. The analysis revealed that nine (60%) of the 15 MPMs showed nuclear and/or cytoplasmic *ZEB1* expression while none of the four normal parietal pleural samples showed detectable levels of *ZEB1* protein (Fig. 6), suggesting the relevant role of *ZEB1* in human MPM.

## DISCUSSION

In the present study we showed that the majority of MPM cell lines express *ZEB1*, and that the transient knockdown of *ZEB1* expression with RNA interference in four MPM cell lines dramatically suppressed their *in vitro* growth. However, stable *ZEB1* knockdown showed less growth inhibitory effects in these MPM cell lines. Gene expression analysis revealed that numerous genes were differentially expressed between transient and stable *ZEB1* knockdown in ACC-MESO-1 cells, including known oncogene *EpCAM*. *EpCAM* knockdown more significantly inhibited growth in ACC-MESO-1 cells expressing sh*ZEB1* than in those expressing sh*GFP*, suggesting that diminished growth inhibition by stable *ZEB1* knockdown may be in part attributable to *EpCAM* up-regulation induced by the *ZEB1* knockdown.

*EpCAM* is shown to be down-regulated by *ZEB1* in breast cancer.<sup>20</sup> We further confirmed this finding in MPM cells. Furthermore, during preparation of this article, Gemmill et al. performed genome-wide expression analysis of lung cancer cell lines and identified *EpCAM* as the gene whose expression most significantly negatively correlates with *ZEB1* expression in non-small cell lung cancer cell lines.<sup>21</sup> These findings suggest that *EpCAM* is a universal target of *ZEB1*, leading us to perform luciferase reporter assay to access the effects of *ZEB1* knockdown on *EpCAM* promoter activity. We found that *EpCAM* promoter activity was increased by *ZEB1* knockdown in H1299 cells, indicating that *ZEB1* negatively regulates *EpCAM* expression by suppressing its promoter activity.

The dramatic growth inhibition by a transient *ZEB1* knockdown in MPM cell lines suggests that a *ZEB1*-targeted therapy for MPM is promising. Nevertheless, we found that stable *ZEB1* did not greatly suppress growth of MPM cells, in part as a result of *EpCAM* up-regulation. Thus, development of a therapeutic strategy that target *ZEB1* must take into account the possibility that gene expression changes resulting from *ZEB1* knockdown may counteract a *ZEB1*-targeted therapy. There are a few possible approaches to address this

issue. One approach is to employ not a long-term but a short-term knockdown of *ZEB1* because the transient *ZEB1* knockdown suppressed growth of MPM cells. However, we observed that the transient *ZEB1* knockdown also up-regulates *EpCAM*, raising the question of why the growth inhibitory effect of a transient *ZEB1* knockdown was not affected by *EpCAM* up-regulation. We speculate that MPM cells may require a certain time period to switch their growth dependency from *ZEB1* to *EpCAM*, and therefore transient *EpCAM* up-regulation does not greatly affect the growth inhibitory effects of the *ZEB1* knockdown. Another approach is to target *ZEB1* and *EpCAM* simultaneously on the basis of our finding that *EpCAM* knockdown efficiently suppresses growth in MPM cells where *ZEB1* is stably suppressed.

Finally, targeting both *ZEB1* and *ZEB2*, another member of the ZEB family genes, seems to be a promising therapeutic strategy for MPM because Gemmill et al. demonstrated that combinatorial knockdown of *ZEB1* and *ZEB2* more significantly reversed mesenchymal to epithelial phenotypes than either alone in lung cancer cells.<sup>21</sup>

In summary, our results showed that a transient *ZEB1* knockdown suppressed growth of MPM cells, suggesting that it may serve as a promising therapeutic target. However, we also found that the growth suppressive effects of *ZEB1* were reduced in a stable knockdown setting, which may be caused by *EpCAM* up-regulation and/or other gene expression changes.

## Supplementary Material

Refer to Web version on PubMed Central for supplementary material.

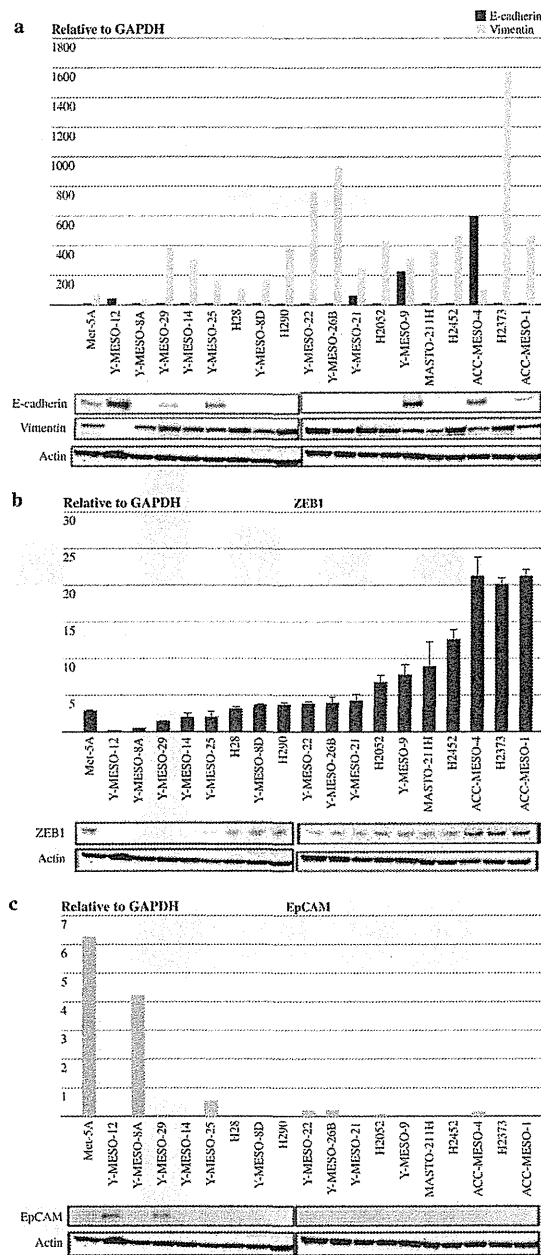
## Acknowledgments

We thank Drs. Thomas Brabletz for providing pSUPER retro-ZEB1 and GFP vectors and Osamu Maeda for giving us technical advice on luciferase reporter assay. This work was supported by Grant-in-Aid for Scientific Research (C) 20590919 (to M.S.), Grant-in-Aid for Scientific Research (C) 20590918 (to M.K.), and Grant-in-Aid for Scientific Research (B) 21390257 (to Y.H.) from the Japan Society for the Promotion of Science, Global COE program at Nagoya University Graduate School of Medicine, which is funded by Japan's Ministry of Education, Culture, Sports, Science and Technology, NCI Special Program of Research Excellence in Lung Cancer (SPORE P50CA70907), and DOD PROSPECT (to J.D.M. and A.F.G.).

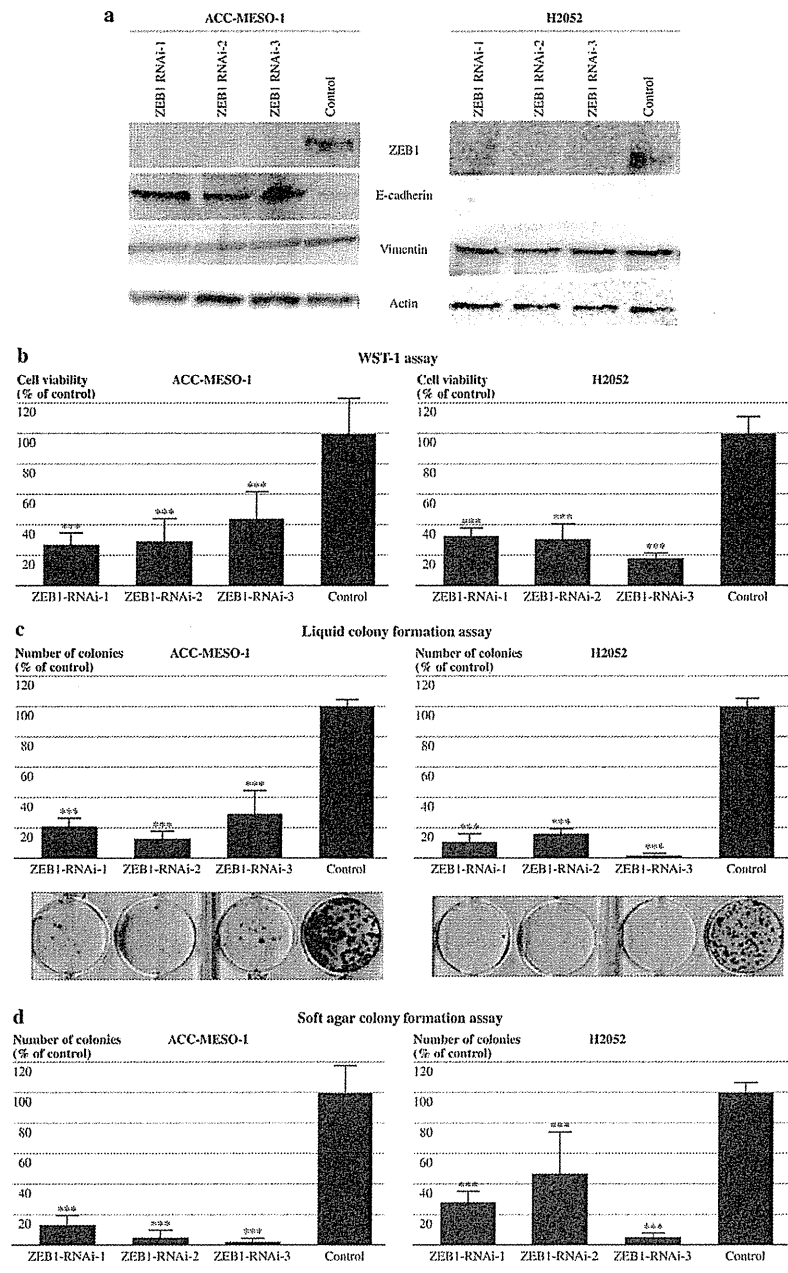
## REFERENCES

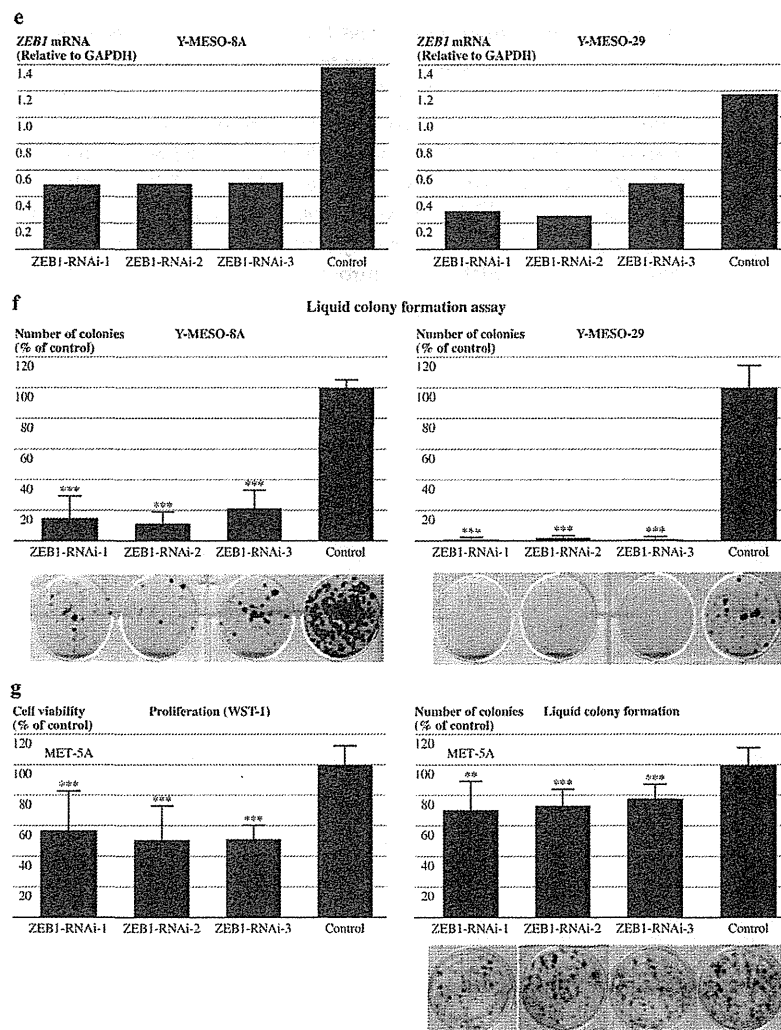
1. Robinson BW, Lake RA. Advances in malignant mesothelioma. *N Engl J Med.* 2005; 353:1591–1603. [PubMed: 16221782]
2. Tsao AS, Wistuba I, Roth JA, Kindler HL. Malignant pleural mesothelioma. *J Clin Oncol.* 2009; 27:2081–2090. [PubMed: 19255316]
3. Voulgari A, Pintzas A. Epithelial-mesenchymal transition in cancer metastasis: mechanisms, markers and strategies to overcome drug resistance in the clinic. *Biochim Biophys Acta.* 2009; 1796:75–90. [PubMed: 19306912]
4. Schramm A, Opitz I, Thies S, et al. Prognostic significance of epithelial–mesenchymal transition in malignant pleural mesothelioma. *Eur J Cardiothorac Surg.* 2010; 37:566–572. [PubMed: 19781955]
5. Peinado H, Olmeda D, Cano A. Snail, Zeb and bHLH factors in tumour progression: an alliance against the epithelial phenotype? *Nat Rev Cancer.* 2007; 7:415–428. [PubMed: 17508028]
6. Schmalhofer O, Brabletz S, Brabletz T. E-cadherin, beta-catenin, and ZEB1 in malignant progression of cancer. *Cancer Metastasis Rev.* 2009; 28:151–166. [PubMed: 19153669]
7. Takeyama Y, Sato M, Horio M, et al. Knockdown of ZEB1, a master epithelial-to-mesenchymal transition (EMT) gene, suppresses anchorage-independent cell growth of lung cancer cells. *Cancer Lett.* 2010; 296:216–224. [PubMed: 20452118]

8. Usami N, Fukui T, Kondo M, et al. Establishment and characterization of four malignant pleural mesothelioma cell lines from Japanese patients. *Cancer Sci.* 2006; 97:387–394. [PubMed: 16630136]
9. Ke Y, Reddel RR, Gerwin BI, et al. Establishment of a human in vitro mesothelial cell model system for investigating mechanisms of asbestos-induced mesothelioma. *Am J Pathol.* 1989; 134:979–991. [PubMed: 2541616]
10. Sato M, Vaughan MB, Girard L, et al. Multiple oncogenic changes (K-RAS(V12), p53 knockdown, mutant EGFRs, p16 bypass, telomerase) are not sufficient to confer a full malignant phenotype on human bronchial epithelial cells. *Cancer Res.* 2006; 66:2116–2128. [PubMed: 16489012]
11. Spaderna S, Schmalhofer O, Wahlbuhl M, et al. The transcriptional repressor ZEB1 promotes metastasis and loss of cell polarity in cancer. *Cancer Res.* 2008; 68:537–544. [PubMed: 18199550]
12. Eger A, Aigner K, Sonderegger S, et al. DeltaEF1 is a transcriptional repressor of E-cadherin and regulates epithelial plasticity in breast cancer cells. *Oncogene.* 2005; 24:2375–2385. [PubMed: 15674322]
13. Tsou JA, Shen LY, Siegmund KD, et al. Distinct DNA methylation profiles in malignant mesothelioma, lung adenocarcinoma, and non-tumor lung. *Lung Cancer.* 2005; 47:193–204. [PubMed: 15639718]
14. Sunaga N, Miyajima K, Suzuki M, et al. Different roles for caveolin-1 in the development of non-small cell lung cancer versus small cell lung cancer. *Cancer Res.* 2004; 64:4277–4285. [PubMed: 15205342]
15. Sunaga N, Shames DS, Girard L, et al. Knockdown of oncogenic KRAS in non-small cell lung cancers suppresses tumor growth and sensitizes tumor cells to targeted therapy. *Mol Cancer Ther.* 2011; 10:336–346. [PubMed: 21306997]
16. Iwanaga K, Yang Y, Raso MG, et al. Pten inactivation accelerates oncogenic K-ras-initiated tumorigenesis in a mouse model of lung cancer. *Cancer Res.* 2008; 68:1119–1127. [PubMed: 18281487]
17. Munz M, Kieu C, Mack B, Schmitt B, Zeidler R, Gires O. The carcinoma-associated antigen EpCAM upregulates c-myc and induces cell proliferation. *Oncogene.* 2004; 23:5748–5758. [PubMed: 15195135]
18. Osta WA, Chen Y, Mikhitarian K, et al. EpCAM is overexpressed in breast cancer and is a potential target for breast cancer gene therapy. *Cancer Res.* 2004; 64:5818–5824. [PubMed: 15313925]
19. Hase T, Sato M, Yoshida K, et al. Pivotal role of epithelial cell adhesion molecule in the survival of lung cancer cells. *Cancer Sci.* 2011; 102:1493–1500. [PubMed: 21535318]
20. Aigner K, Dampier B, Descovich L, et al. The transcription factor ZEB1 (deltaEF1) promotes tumour cell dedifferentiation by repressing master regulators of epithelial polarity. *Oncogene.* 2007; 26:6979–6988. [PubMed: 17486063]
21. Gemmill RM, Roche J, Potiron VA, et al. ZEB1-responsive genes in non-small cell lung cancer. *Cancer Lett.* 2011; 300:66–78. [PubMed: 20980099]



**FIG. 1.** Most MPM cell lines exhibit mesenchymal phenotype (low E-cadherin/high vimentin) and express ZEB1. qRT-PCR (*top*) and Western blot testing (*bottom*) analyses of E-cadherin, vimentin (a), ZEB1 (b), and EpCAM (c) in 18 MPM cell lines and the immortalized pleural mesothelioma line MeT-5A (control)

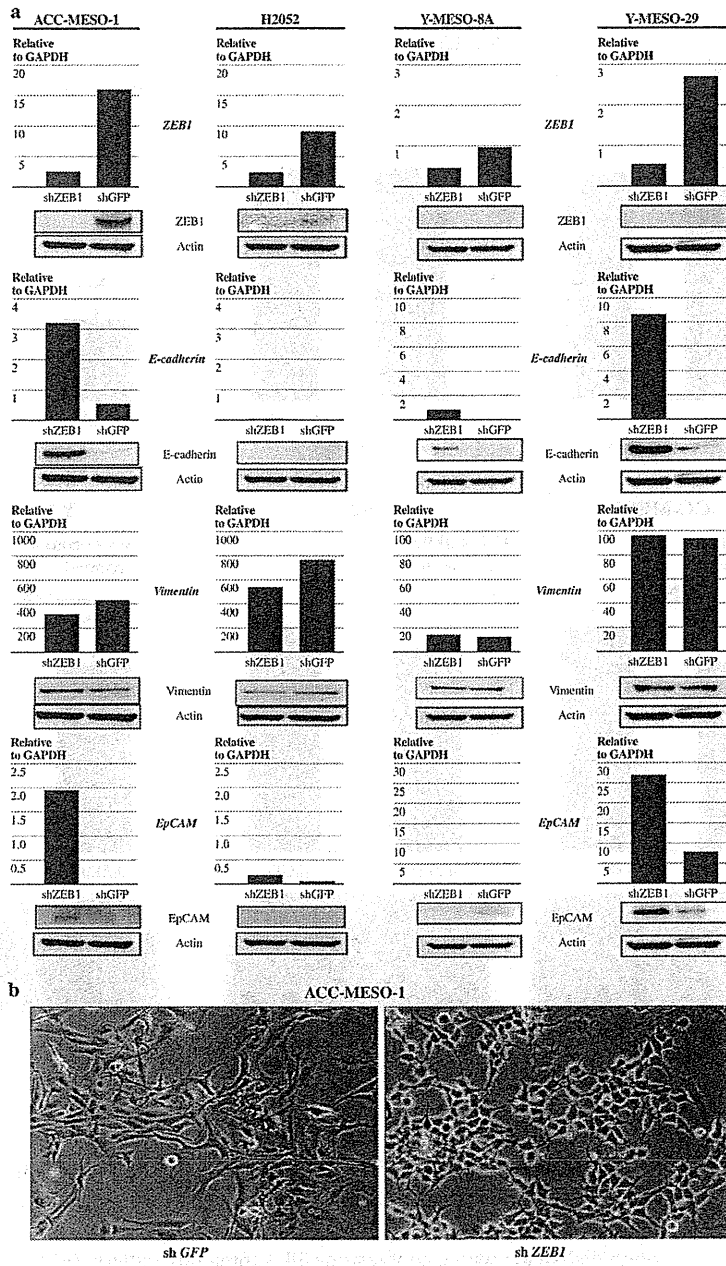


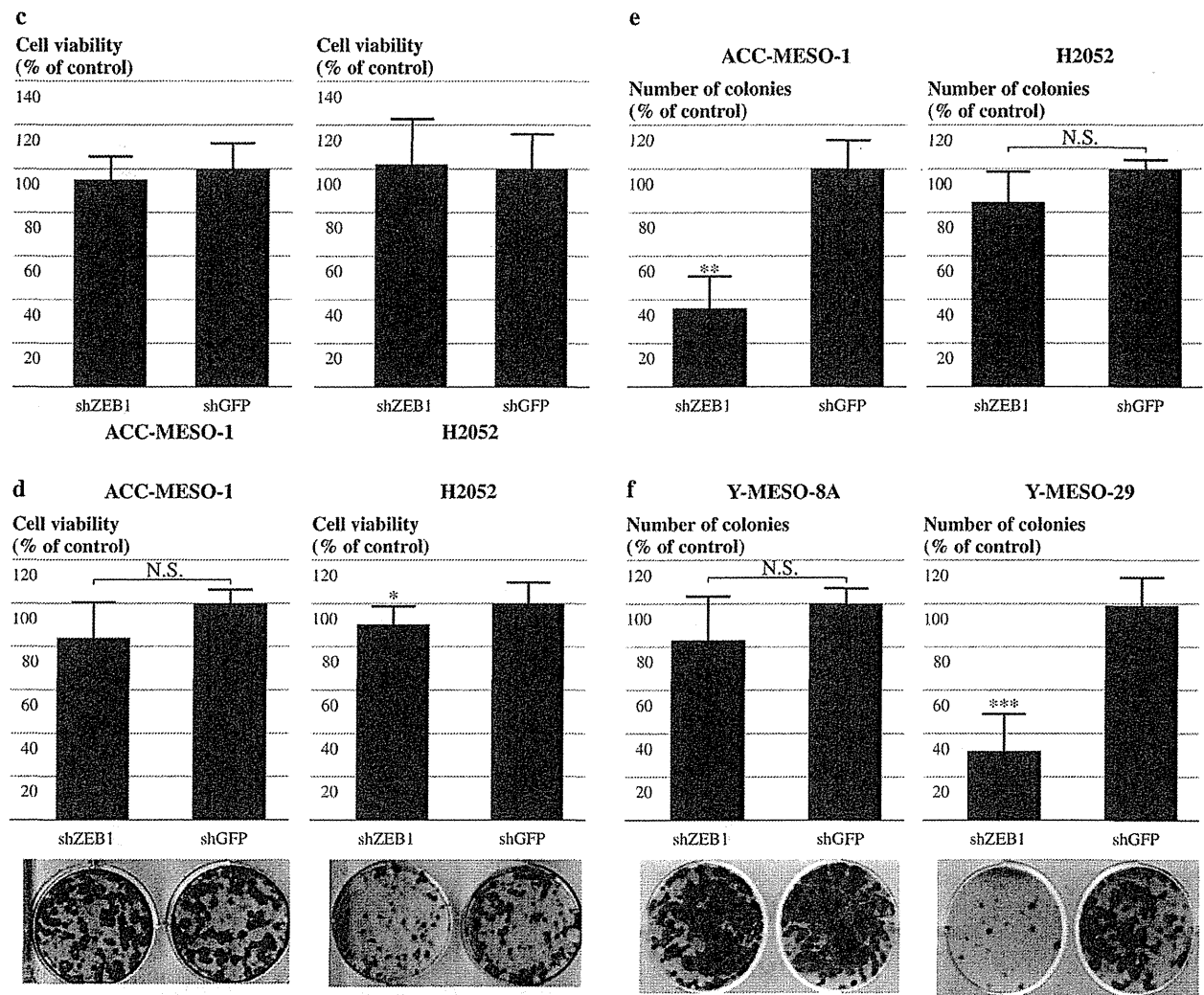


**FIG. 2.** Transient *ZEB1* knockdown suppresses cellular proliferation and liquid and soft agar colony formation in MPM cell lines. (a) Western blots of *ZEB1*, E-cadherin, and vimentin in ACC-MESO-1 and H2052 transfected with *ZEB1* knockdown siRNA or control oligos. Actin was used as a loading control. (b) Cell proliferation (WST-1) assay for ACC-MESO-1 and H2052 cells transfected with *ZEB1* knockdown siRNA or control oligos. Cells were transfected with 3 different siRNA oligos targeting *ZEB1* or control oligos. Cells were counted 48 h after transfection, and 1000 cells were plated in 96-well plates. Absorbance values were determined 96 h after transfection. Results are from 3 independent experiments with 8 replicates each and shown as mean  $\pm$  SD. Values of cells transfected with control oligos are set as 100%. (c) Liquid colony formation assay of ACC-MESO-1 and H2052 cells transfected with *ZEB1* knockdown siRNA or control oligos. Cells were counted 48 h after transfection, and 500 to 1000 cells were plated in 6-well plates in triplicate, cultured for 2 weeks, and stained with methylene blue. Colonies  $>2$  mm were counted. Results are from 3 independent experiments and shown as mean  $\pm$  SD. Colony numbers of cells transfected with control oligos are set as 100%. (d) Soft agar colony formation assay for ACC-MESO-1 and H2052 cells transfected with *ZEB1* knockdown siRNA or control oligos. Cells were

counted 48 h after transfection, and 1000 cells were suspended in 0.37% SeaKem GTG Agarose (Lonza, Rockland, ME) in triplicate 12-well plates. About 2 weeks later, colonies (>50 cells) were counted. Results from 3 independent experiments are shown as mean  $\pm$  SD. Colony numbers of cells transfected with control oligos are set as 100%. (e) qRT-PCR analysis of *ZEB1*, *E-cadherin*, and *vimentin* in Y-MESO-8A and Y-MESO-29 transfected with *ZEB1* knockdown siRNA or control oligos. (f) Liquid colony formation assay of Y-MESO-8A and Y-MESO-29 cells transfected with *ZEB1* knockdown siRNA or control oligos. (g) WST1 and liquid colony formation assays of MeT-5A cells transfected with *ZEB1* knockdown siRNA or control oligos. \*\* $P < 0.01$ , \*\*\* $P < 0.001$  (Mann–Whitney *U*-test)





**FIG. 3.**

Stable knockdown of *ZEB1* inhibits growth only modestly or not at all in malignant mesothelioma cell lines. (a) qRT-PCR analysis of *E-cadherin*, *vimentin*, *ZEB1*, and *EpCAM* in ACC-MESO-1, H2052, Y-MESO-8A and Y-MESO-29 cells transfected with sh*ZEB1* or sh*GFP* vectors. (b) Photomicrographs of ACC-MESO-1 cells transfected with sh*ZEB1* or sh*GFP* vectors. Note that ACC-MESO-1 cells transfected with sh*ZEB1* vector exhibit an epithelial shape with a cobblestone-like spreading pattern. (c) Cell proliferation (WST-1) assay for ACC-MESO-1 and H2052 cells transfected with sh*ZEB1* or sh*GFP* vectors. The results are averages of 3 independent experiments. (d) Liquid colony formation assay for ACC-MESO-1 and H2052 cells transfected with sh*ZEB1* or sh*GFP* vectors. The results are averages of 3 independent experiments. \* $P < 0.05$  (Mann-Whitney *U*-test) (e) Soft agar colony formation assay of ACC-MESO-1 and H2052 cells transfected with sh*ZEB1* or sh*GFP* vectors. (f) Liquid colony formation assay for Y-MESO-8A and Y-MESO-29 cells transfected with sh*ZEB1* or sh*GFP* vectors. The results are averages of 2 or 3 independent experiments. \*\* $P < 0.01$  (Mann-Whitney *U*-test)

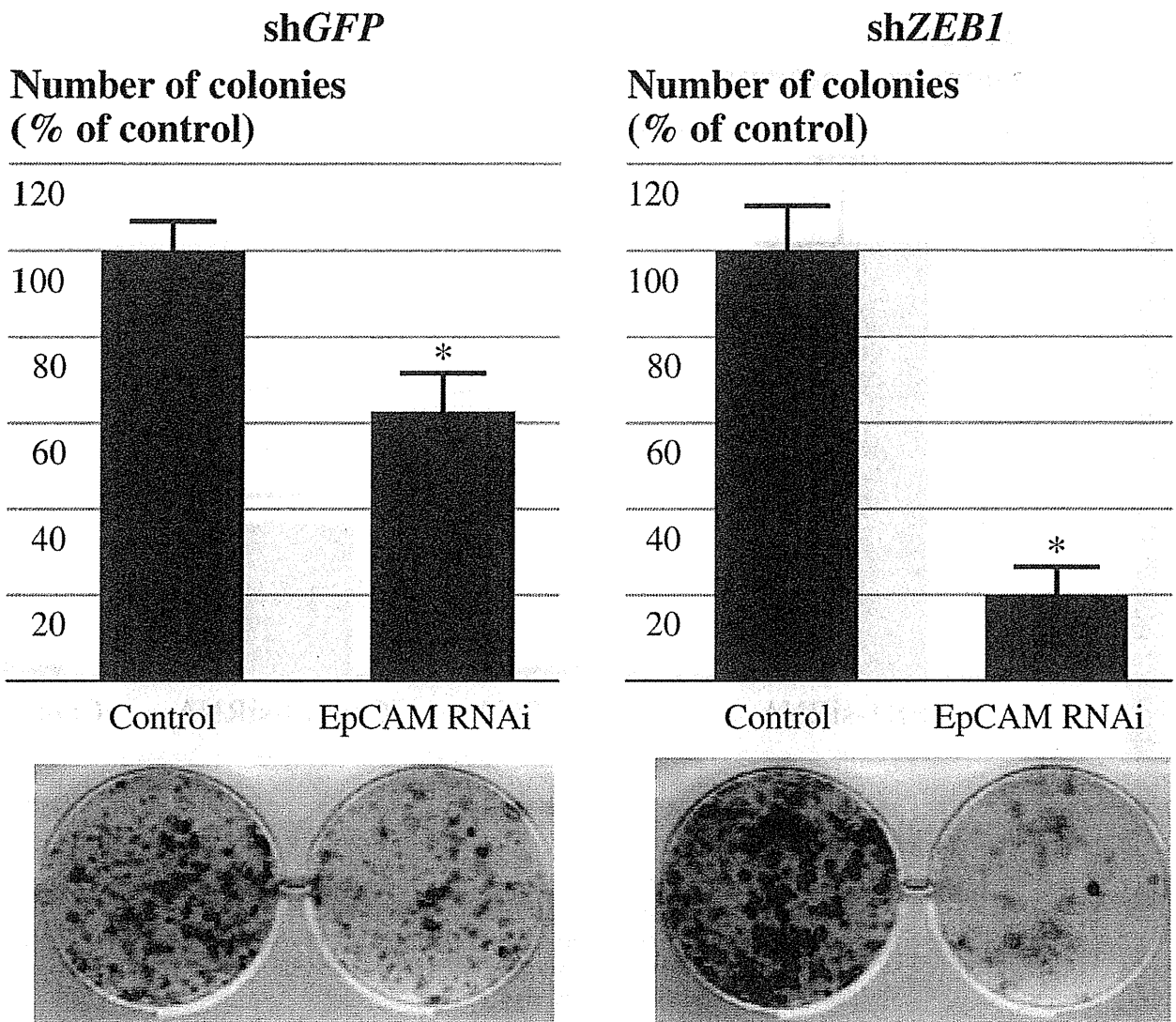


**FIG. 4.** *EpCAM* knockdown suppresses liquid colony formation of ACC-MESO-1 cells more prominently in those expressing *shZEB1* than in those expressing *shGFP*. Liquid colony formation assay for ACC-MESO-1 cells expressing *shZEB1* or *shGFP* vectors transiently transfected with *EpCAM* siRNA or control oligos. Cells expressing *shZEB1* or *shGFP* vectors were transiently transfected with *EpCAM* siRNA or control oligos. A thousand cells were plated in 6-well plates in triplicate 48 h after transfection, cultured for 2 weeks, and stained with methylene blue. Colonies >2 mm were counted. Results are from 3 independent experiments and shown as mean  $\pm$  SD. Numbers of control cell colonies are set as 100%. \* $P < 0.001$  (Mann-Whitney *U*-test)

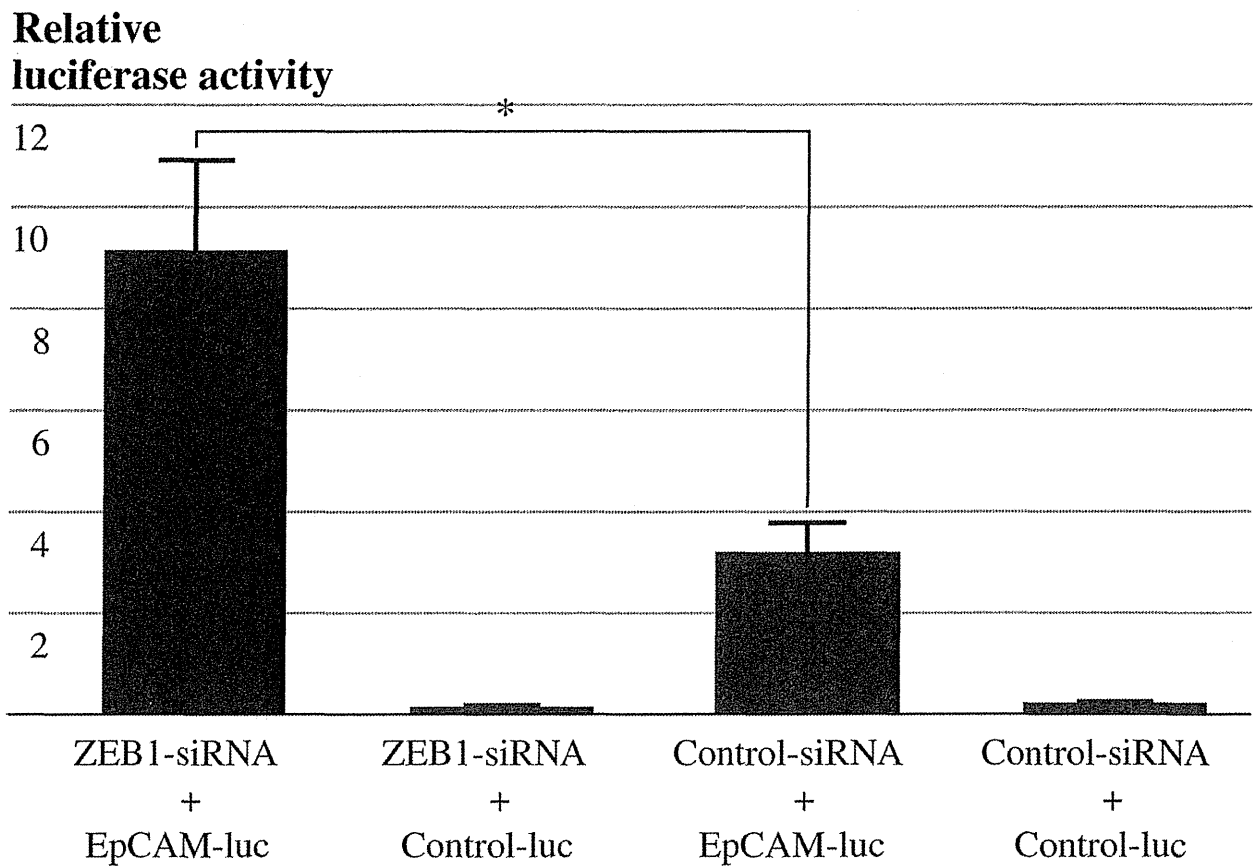


**FIG. 5.** *ZEB1* suppresses *EpCAM* mRNA expression through repressing *EpCAM* promoter activity. *ZEB1* or control siRNA-transfected H1299 cells were transfected with TACSTD1 (*EpCAM*)-PROM firefly luciferase vector or pGL4.11 control vector and phRL-TK renilla luciferase vector. The ratios of firefly/renilla luciferase activities are shown. Representative data from 3 independent experiments are shown. \* $P < 0.05$